Observation of Gravitational Waves from a Binary Black Hole Merger

B. P. Abbott,[1] R. Abbott,[1] T. D. Abbott,[2] M. R. Abernathy,[1] F. Acernese,[3,4] K. Ackley,[5] C. Adams,[6] T. Adams,[7] P. Addesso,[8] R. X. Adhikari,[1] V. B. Adya,[9] C. Affeldt,[9] M. Agathos,[10] K. Agatsuma,[10] N. Aggarwal,[11] O. D. Aguiar,[12] L. Aiello,[13,14] A. Ain,[15] P. Ajith,[16] B. Allen,[9,17,18] A. Allocca,[19,20] P. A. Altin,[21] D. V. Amariutei,[5] S. B. Anderson,[1] W. G. Anderson,[17] K. Arai,[1] M. A. Arain,[5] M. C. Araya,[1] C. C. Arceneaux,[22] J. S. Areeda,[23] N. Arnaud,[24] K. G. Arun,[25] S. Ascenzi,[26,14] G. Ashton,[27] M. Ast,[28] S. M. Aston,[6] P. Astone,[29] P. Aufmuth,[18] C. Aulbert,[9] S. Babak,[30] P. Bacon,[31] M. K. M. Bader,[10] P. T. Baker,[32] F. Baldaccini,[33,34] G. Ballardin,[35] S. W. Ballmer,[36] J. C. Barayoga,[1] S. E. Barclay,[37] B. C. Barish,[1] D. Barker,[38] F. Barone,[3,4] B. Barr,[37] L. Barsotti,[11] M. Barsuglia,[31] D. Barta,[39] J. Bartlett,[38] M. A. Barton,[38] I. Bartos,[40] R. Bassiri,[41] A. Basti,[19,20] J. C. Batch,[38] C. Baune,[9] V. Bavigadda,[35] M. Bazzan,[42,43] B. Behnke,[30] M. Bejger,[44] C. Belczynski,[45] A. S. Bell,[37] C. J. Bell,[37] B. K. Berger,[1] J. Bergman,[38] G. Bergmann,[9] C. P. L. Berry,[46] D. Bersanetti,[47,48] A. Bertolini,[10] J. Betzwieser,[6] S. Bhagwat,[36] R. Bhandare,[49] I. A. Bilenko,[50] G. Billingsley,[1] J. Birch,[6] R. Birney,[51] O. Birnholtz,[9] S. Biscans,[11] A. Bisht,[9,18] M. Bitossi,[35] C. Biwer,[36] M. A. Bizouard,[24] J. K. Blackburn,[1] C. D. Blair,[52] D. Blair,[52] R. M. Blair,[38] S. Bloemen,[53] O. Bock,[9] T. P. Bodiya,[11] M. Boer,[54] G. Bogaert,[54] C. Bogan,[9] A. Bohe,[30] P. Bojtos,[55] C. Bond,[46] F. Bondu,[56] R. Bonnand,[7] B. A. Boom,[10] R. Bork,[1] V. Boschi,[19,20] S. Bose,[57,15] Y. Bouffanais,[31] A. Bozzi,[35] C. Bradaschia,[20] P. R. Brady,[17] V. B. Braginsky,[50] M. Branchesi,[58,59] J. E. Brau,[60] T. Briant,[61] A. Brillet,[54] M. Brinkmann,[9] V. Brisson,[24] P. Brockill,[17] A. F. Brooks,[1] D. A. Brown,[36] D. D. Brown,[46] N. M. Brown,[11] C. C. Buchanan,[2] A. Buikema,[11] T. Bulik,[45] H. J. Bulten,[62,10] A. Buonanno,[30,63] D. Buskulic,[7] C. Buy,[31] R. L. Byer,[41] M. Cabero,[9] L. Cadonati,[64] G. Cagnoli,[65,66] C. Cahillane,[1] J. Calderón Bustillo,[67,64] T. Callister,[1] E. Calloni,[68,4] J. B. Camp,[69] K. C. Cannon,[70] J. Cao,[71] C. D. Capano,[9] E. Capocasa,[31] F. Carbognani,[35] S. Caride,[72] J. Casanueva Diaz,[24] C. Casentini,[26,14] S. Caudill,[17] M. Cavaglià,[22] F. Cavalier,[24] R. Cavalieri,[35] G. Cella,[20] C. Cepeda,[1] L. Cerboni Baiardi,[58,59] G. Cerretani,[19,20] E. Cesarini,[26,14] R. Chakraborty,[1] T. Chalermsongsak,[1] S. J. Chamberlin,[17] M. Chan,[37] S. Chao,[73] P. Charlton,[74] E. Chassande-Mottin,[31] H. Y. Chen,[75] Y. Chen,[76] C. Cheng,[73] A. Chincarini,[48] A. Chiummo,[35] H. S. Cho,[77] M. Cho,[63] J. H. Chow,[21] N. Christensen,[78] Q. Chu,[52] S. Chua,[61] S. Chung,[52] G. Ciani,[5] F. Clara,[38] J. A. Clark,[64] F. Cleva,[54] E. Coccia,[26,13,14] P.-F. Cohadon,[61] A. Colla,[79,29] C. G. Collette,[80] M. Constancio Jr.,[12] A. Conte,[79,29] L. Conti,[43] D. Cook,[38] T. R. Corbitt,[2] N. Cornish,[32] A. Corsi,[81] S. Cortese,[35] C. A. Costa,[12] M. W. Coughlin,[78] S. B. Coughlin,[82] J.-P. Coulon,[54] S. T. Countryman,[40] P. Couvares,[1] D. M. Coward,[52] M. J. Cowart,[6] D. C. Coyne,[1] R. Coyne,[81] K. Craig,[37] J. D. E. Creighton,[17] J. Cripe,[2] S. G. Crowder,[83] A. M. Cruise,[46] A. Cumming,[37] L. Cunningham,[37] E. Cuoco,[35] T. Dal Canton,[9] S. L. Danilishin,[37] S. D'Antonio,[14] K. Danzmann,[18,9] N. S. Darman,[84] C. F. Da Silva Costa,[5] V. Dattilo,[35] I. Dave,[49] H. P. Daveloza,[85] M. Davier,[24] G. S. Davies,[37] E. J. Daw,[86] R. Day,[35] S. De,[36] D. DeBra,[41] G. Debreczeni,[39] J. Degallaix,[66] M. De Laurentis,[68,4] S. Deléglise,[61] W. Del Pozzo,[46] T. Denker,[9,18] T. Dent,[9] H. Dereli,[54] V. Dergachev,[1] R. DeRosa,[6] R. De Rosa,[68,4] R. DeSalvo,[8] S. Dhurandhar,[15] M. C. Díaz,[85] L. Di Fiore,[4] M. Di Giovanni,[79,29] A. Di Lieto,[19,20] S. Di Pace,[79,29] I. Di Palma,[30,9] A. Di Virgilio,[20] G. Dojcinoski,[87] V. Dolique,[66] F. Donovan,[11] K. L. Dooley,[22] S. Doravari,[6] R. Douglas,[37] T. P. Downes,[17] M. Drago,[9,88,89] R. W. P. Drever,[1] J. C. Driggers,[38] Z. Du,[71] M. Ducrot,[7] S. E. Dwyer,[38] T. B. Edo,[86] M. C. Edwards,[78] A. Effler,[6] H.-B. Eggenstein,[9] P. Ehrens,[1] J. M. Eichholz,[5] S. S. Eikenberry,[5] W. Engels,[76] R. C. Essick,[11] T. Etzel,[1] M. Evans,[11] T. M. Evans,[6] R. Everett,[90] M. Factourovich,[40] V. Fafone,[26,14,13] H. Fair,[36] S. Fairhurst,[82] X. Fan,[71] Q. Fang,[52] S. Farinon,[48] B. Farr,[75] W. M. Farr,[46] M. Favata,[87] M. Fays,[82] H. Fehrmann,[9] M. M. Fejer,[41] D. Feldbaum,[5] I. Ferrante,[19,20] E. C. Ferreira,[12] F. Ferrini,[35] F. Fidecaro,[19,20] L. S. Finn,[90] I. Fiori,[35] D. Fiorucci,[31] R. P. Fisher,[36] R. Flaminio[§,66] M. Fletcher,[37] H. Fong,[70] J.-D. Fournier,[54] S. Franco,[24] S. Frasca,[79,29] F. Frasconi,[20] M. Frede,[9] Z. Frei,[55] A. Freise,[46] R. Frey,[60] V. Frey,[24] T. T. Fricke,[9] P. Fritschel,[11] V. V. Frolov,[6] P. Fulda,[5] M. Fyffe,[6] H. A. G. Gabbard,[22] J. R. Gair,[91] L. Gammaitoni,[33,34] S. G. Gaonkar,[15] F. Garufi,[68,4] A. Gatto,[31] G. Gaur,[92,93] N. Gehrels,[69] G. Gemme,[48] B. Gendre,[54] E. Genin,[35] A. Gennai,[20] J. George,[49] L. Gergely,[94] V. Germain,[7] A. Ghosh,[16] A. Ghosh,[16] S. Ghosh,[53,10] J. A. Giaime,[2,6] K. D. Giardina,[6] A. Giazotto,[20] K. Gill,[95] A. Glaefke,[37] J. R. Gleason,[5] E. Goetz,[72] R. Goetz,[5] L. Gondan,[55] G. González,[2] J. M. Gonzalez Castro,[19,20] A. Gopakumar,[96] N. A. Gordon,[37] M. L. Gorodetsky,[50] S. E. Gossan,[1] M. Gosselin,[35] R. Gouaty,[7] C. Graef,[37] P. B. Graff,[69,63] M. Granata,[66] A. Grant,[37] S. Gras,[11] C. Gray,[38] G. Greco,[58,59] A. C. Green,[46] R. J. S. Greenhalgh,[97] P. Groot,[53] H. Grote,[9] S. Grunewald,[30] G. M. Guidi,[58,59] X. Guo,[71] A. Gupta,[15] M. K. Gupta,[93] K. E. Gushwa,[1] E. K. Gustafson,[1] R. Gustafson,[72] J. J. Hacker,[23] B. R. Hall,[57] E. D. Hall,[1] G. Hammond,[37] M. Haney,[96] M. M. Hanke,[9] J. Hanks,[38] C. Hanna,[90] M. D. Hannam,[82] J. Hanson,[6] T. Hardwick,[2] J. Harms,[58,59] G. M. Harry,[98] I. W. Harry,[30] M. J. Hart,[37] M. T. Hartman,[5] C.-J. Haster,[46] K. Haughian,[37] J. Healy,[99] J. Heefner[*,1] A. Heidmann,[61] M. C. Heintze,[5,6] H. Heitmann,[54] P. Hello,[24] G. Hemming,[35] M. Hendry,[37]

I. S. Heng,[37] J. Hennig,[37] A. W. Heptonstall,[1] M. Heurs,[9,18] S. Hild,[37] D. Hoak,[100] K. A. Hodge,[1] D. Hofman,[66] S. E. Hollitt,[101] K. Holt,[6] D. E. Holz,[75] P. Hopkins,[82] D. J. Hosken,[101] J. Hough,[37] E. A. Houston,[37] E. J. Howell,[52] Y. M. Hu,[37] S. Huang,[73] E. A. Huerta,[102] D. Huet,[24] B. Hughey,[95] S. Husa,[67] S. H. Huttner,[37] T. Huynh-Dinh,[6] A. Idrisy,[90] N. Indik,[9] D. R. Ingram,[38] R. Inta,[81] H. N. Isa,[37] J.-M. Isac,[61] M. Isi,[1] G. Islas,[23] T. Isogai,[11] B. R. Iyer,[16] K. Izumi,[38] M. B. Jacobson,[1] T. Jacqmin,[61] H. Jang,[77] K. Jani,[64] P. Jaranowski,[103] S. Jawahar,[104] F. Jiménez-Forteza,[67] W. W. Johnson,[2] N. K. Johnson-McDaniel,[16] D. I. Jones,[27] R. Jones,[37] R. J. G. Jonker,[10] L. Ju,[52] Haris K,[105] C. V. Kalaghatgi,[25] V. Kalogera,[106] S. Kandhasamy,[22] G. Kang,[77] J. B. Kanner,[1] S. Karki,[60] M. Kasprzack,[2,24,35] E. Katsavounidis,[11] W. Katzman,[6] S. Kaufer,[18] T. Kaur,[52] K. Kawabe,[38] F. Kawazoe,[9] F. Kéfélian,[54] M. S. Kehl,[70] D. Keitel,[9] D. B. Kelley,[36] W. Kells,[1] R. Kennedy,[86] D. G. Keppel,[9] J. S. Key,[85] A. Khalaidovski,[9] F. Y. Khalili,[50] I. Khan,[13] S. Khan,[82] Z. Khan,[93] E. A. Khazanov,[107] N. Kijbunchoo,[38] C. Kim,[77] J. Kim,[108] K. Kim,[109] N. Kim,[77] N. Kim,[41] Y.-M. Kim,[108] E. J. King,[101] P. J. King,[38] D. L. Kinzel,[6] J. S. Kissel,[38] L. Kleybolte,[28] S. Klimenko,[5] S. M. Koehlenbeck,[9] K. Kokeyama,[2] S. Koley,[10] V. Kondrashov,[1] A. Kontos,[11] S. Koranda,[17] M. Korobko,[28] W. Z. Korth,[1] I. Kowalska,[45] D. B. Kozak,[1] V. Kringel,[9] B. Krishnan,[9] A. Królak,[110,111] C. Krueger,[18] G. Kuehn,[9] P. Kumar,[70] R. Kumar,[37] L. Kuo,[73] A. Kutynia,[110] P. Kwee,[11] B. D. Lackey,[36] M. Landry,[38] J. Lange,[99] B. Lantz,[41] P. D. Lasky,[112] A. Lazzarini,[1] C. Lazzaro,[64,43] P. Leaci,[30,79,29] S. Leavey,[37] E. O. Lebigot,[31,71] C. H. Lee,[108] H. K. Lee,[109] H. M. Lee,[113] K. Lee,[37] A. Lenon,[36] M. Leonardi,[88,89] J. R. Leong,[9] N. Leroy,[24] N. Letendre,[7] Y. Levin,[112] B. M. Levine,[38] T. G. F. Li,[1] A. Libson,[11] T. B. Littenberg,[106] N. A. Lockerbie,[104] J. Logue,[37] A. L. Lombardi,[100] L. T. London,[82] J. E. Lord,[36] M. Lorenzini,[13,14] V. Loriette,[114] M. Lormand,[6] G. Losurdo,[59] J. D. Lough,[9,18] C. O. Lousto,[99] G. Lovelace,[23] H. Lück,[18,9] A. P. Lundgren,[9] J. Luo,[78] R. Lynch,[11] Y. Ma,[52] T. MacDonald,[41] B. Machenschalk,[9] M. MacInnis,[11] D. M. Macleod,[2] F. Magaña-Sandoval,[36] R. M. Magee,[57] M. Mageswaran,[1] E. Majorana,[29] I. Maksimovic,[114] V. Malvezzi,[26,14] N. Man,[54] I. Mandel,[46] V. Mandic,[83] V. Mangano,[37] G. L. Mansell,[21] M. Manske,[17] M. Mantovani,[35] F. Marchesoni,[115,34] F. Marion,[7] S. Márka,[40] Z. Márka,[40] A. S. Markosyan,[41] E. Maros,[1] F. Martelli,[58,59] L. Martellini,[54] I. W. Martin,[37] R. M. Martin,[5] D. V. Martynov,[1] J. N. Marx,[1] K. Mason,[11] A. Masserot,[7] T. J. Massinger,[36] M. Masso-Reid,[37] F. Matichard,[11] L. Matone,[40] N. Mavalvala,[11] N. Mazumder,[57] G. Mazzolo,[9] R. McCarthy,[38] D. E. McClelland,[21] S. McCormick,[6] S. C. McGuire,[116] G. McIntyre,[1] J. McIver,[100] D. J. McManus,[21] S. T. McWilliams,[102] D. Meacher,[54] G. D. Meadors,[30,9] J. Meidam,[10] A. Melatos,[84] G. Mendell,[38] D. Mendoza-Gandara,[9] R. A. Mercer,[17] E. Merilh,[38] M. Merzougui,[54] S. Meshkov,[1] C. Messenger,[37] C. Messick,[90] P. M. Meyers,[83] F. Mezzani,[29,79] H. Miao,[46] C. Michel,[66] H. Middleton,[46] E. E. Mikhailov,[117] L. Milano,[68,4] J. Miller,[11] M. Millhouse,[32] Y. Minenkov,[14] J. Ming,[30,9] S. Mirshekari,[118] C. Mishra,[16] S. Mitra,[15] V. P. Mitrofanov,[50] G. Mitselmakher,[5] R. Mittleman,[11] A. Moggi,[20] M. Mohan,[35] S. R. P. Mohapatra,[11] M. Montani,[58,59] B. C. Moore,[87] C. J. Moore,[119] D. Moraru,[38] G. Moreno,[38] S. R. Morriss,[85] K. Mossavi,[9] B. Mours,[7] C. M. Mow-Lowry,[46] C. L. Mueller,[5] G. Mueller,[5] A. W. Muir,[82] Arunava Mukherjee,[16] D. Mukherjee,[17] S. Mukherjee,[85] A. Mullavey,[6] J. Munch,[101] D. J. Murphy,[40] P. G. Murray,[37] A. Mytidis,[5] I. Nardecchia,[26,14] L. Naticchioni,[79,29] R. K. Nayak,[120] V. Necula,[5] K. Nedkova,[100] G. Nelemans,[53,10] M. Neri,[47,48] A. Neunzert,[72] G. Newton,[37] T. T. Nguyen,[21] A. B. Nielsen,[9] S. Nissanke,[53,10] A. Nitz,[9] F. Nocera,[35] D. Nolting,[6] M. E. N. Normandin,[85] L. K. Nuttall,[36] J. Oberling,[38] E. Ochsner,[17] J. O'Dell,[97] E. Oelker,[11] G. H. Ogin,[121] J. J. Oh,[122] S. H. Oh,[122] F. Ohme,[82] M. Oliver,[67] P. Oppermann,[9] Richard J. Oram,[6] B. O'Reilly,[6] R. O'Shaughnessy,[99] C. D. Ott,[76] D. J. Ottaway,[101] R. S. Ottens,[5] H. Overmier,[6] B. J. Owen,[81] A. Pai,[105] S. A. Pai,[49] J. R. Palamos,[60] O. Palashov,[107] C. Palomba,[29] A. Pal-Singh,[28] H. Pan,[73] Y. Pan,[63] C. Pankow,[17,106] F. Pannarale,[82] B. C. Pant,[49] F. Paoletti,[35,20] A. Paoli,[35] M. A. Papa,[30,17,9] H. R. Paris,[41] W. Parker,[6] D. Pascucci,[37] A. Pasqualetti,[35] R. Passaquieti,[19,20] D. Passuello,[20] B. Patricelli,[19,20] Z. Patrick,[41] B. L. Pearlstone,[37] M. Pedraza,[1] R. Pedurand,[66] L. Pekowsky,[36] A. Pele,[6] S. Penn,[123] R. Pereira,[40] A. Perreca,[1] H. P. Pfeiffer,[70,9] M. Phelps,[37] O. Piccinni,[79,29] M. Pichot,[54] M. Pickenpack,[9] F. Piergiovanni,[58,59] V. Pierro,[8] G. Pillant,[35] L. Pinard,[66] I. M. Pinto,[8] M. Pitkin,[37] J. H. Poeld,[9] R. Poggiani,[19,20] P. Popolizio,[35] A. Post,[9] J. Powell,[37] J. Prasad,[15] V. Predoi,[82] S. S. Premachandra,[112] T. Prestegard,[83] L. R. Price,[1] M. Prijatelj,[35] M. Principe,[8] S. Privitera,[30] R. Prix,[9] G. A. Prodi,[88,89] L. Prokhorov,[50] O. Puncken,[9] M. Punturo,[34] P. Puppo,[29] M. Pürrer,[82] H. Qi,[17] J. Qin,[52] V. Quetschke,[85] E. A. Quintero,[1] R. Quitzow-James,[60] F. J. Raab,[38] D. S. Rabeling,[21] H. Radkins,[38] P. Raffai,[55] S. Raja,[49] M. Rakhmanov,[85] C. R. Ramet,[6] P. Rapagnani,[79,29] V. Raymond,[30] M. Razzano,[19,20] V. Re,[26] J. Read,[23] C. M. Reed,[38] T. Regimbau,[54] L. Rei,[48] S. Reid,[51] D. H. Reitze,[1,5] H. Rew,[117] S. D. Reyes,[36] F. Ricci,[79,29] K. Riles,[72] N. A. Robertson,[1,37] R. Robie,[37] F. Robinet,[24] A. Rocchi,[14] L. Rolland,[7] J. G. Rollins,[1] V. J. Roma,[60] J. D. Romano,[85] R. Romano,[3,4] G. Romanov,[117] J. H. Romie,[6] D. Rosińska,[124,44] S. Rowan,[37] A. Rüdiger,[9] P. Ruggi,[35] K. Ryan,[38] S. Sachdev,[1] T. Sadecki,[38] L. Sadeghian,[17] L. Salconi,[35] M. Saleem,[105] F. Salemi,[9]

A. Samajdar,[120] L. Sammut,[84] E. J. Sanchez,[1] V. Sandberg,[38] B. Sandeen,[106] G. H. Sanders,[1] J. R. Sanders,[72] B. Sassolas,[66] B. S. Sathyaprakash,[82] P. R. Saulson,[36] O. Sauter,[72] R. L. Savage,[38] A. Sawadsky,[18] P. Schale,[60] R. Schilling[†],[9] J. Schmidt,[9] P. Schmidt,[1,76] R. Schnabel,[28] R. M. S. Schofield,[60] A. Schönbeck,[28] E. Schreiber,[9] D. Schuette,[9,18] B. F. Schutz,[82] J. Scott,[37] S. M. Scott,[21] D. Sellers,[6] D. Sentenac,[35] V. Sequino,[26,14] A. Sergeev,[107] G. Serna,[23] Y. Setyawati,[53,10] A. Sevigny,[38] D. A. Shaddock,[21] S. Shah,[53,10] M. S. Shahriar,[106] M. Shaltev,[9] Z. Shao,[1] B. Shapiro,[41] P. Shawhan,[63] A. Sheperd,[17] D. H. Shoemaker,[11] D. M. Shoemaker,[64] K. Siellez,[54] X. Siemens,[17] D. Sigg,[38] A. D. Silva,[12] D. Simakov,[9] A. Singer,[1] L. P. Singer,[69] A. Singh,[30,9] R. Singh,[2] A. Singhal,[13] A. M. Sintes,[67] B. J. J. Slagmolen,[21] J. R. Smith,[23] M. R. Smith,[1] N. D. Smith,[1] R. J. E. Smith,[1] E. J. Son,[122] B. Sorazu,[37] F. Sorrentino,[48] T. Souradeep,[15] A. K. Srivastava,[93] A. Staley,[40] M. Steinke,[9] J. Steinlechner,[37] S. Steinlechner,[37] D. Steinmeyer,[9,18] B. C. Stephens,[17] S. P. Stevenson,[46] R. Stone,[85] K. A. Strain,[37] N. Straniero,[66] G. Stratta,[58,59] N. A. Strauss,[78] S. Strigin,[50] R. Sturani,[118] A. L. Stuver,[6] T. Z. Summerscales,[125] L. Sun,[84] P. J. Sutton,[82] B. L. Swinkels,[35] M. J. Szczepanczyk,[95] M. Tacca,[31] D. Talukder,[60] D. B. Tanner,[5] M. Tápai,[94] S. P. Tarabrin,[9] A. Taracchini,[30] R. Taylor,[1] T. Theeg,[9] M. P. Thirugnanasambandam,[1] E. G. Thomas,[46] M. Thomas,[6] P. Thomas,[38] K. A. Thorne,[6] K. S. Thorne,[76] E. Thrane,[112] S. Tiwari,[13] V. Tiwari,[82] K. V. Tokmakov,[104] C. Tomlinson,[86] M. Tonelli,[19,20] C. V. Torres[‡],[85] C. I. Torrie,[1] D. Töyrä,[46] F. Travasso,[33,34] G. Traylor,[6] D. Trifirò,[22] M. C. Tringali,[88,89] L. Trozzo,[126,20] M. Tse,[11] M. Turconi,[54] D. Tuyenbayev,[85] D. Ugolini,[127] C. S. Unnikrishnan,[96] A. L. Urban,[17] S. A. Usman,[36] H. Vahlbruch,[18] G. Vajente,[1] G. Valdes,[85] M. Vallisneri,[76] N. van Bakel,[10] M. van Beuzekom,[10] J. F. J. van den Brand,[62,10] C. Van Den Broeck,[10] D. C. Vander-Hyde,[36,23] L. van der Schaaf,[10] J. V. van Heijningen,[10] A. A. van Veggel,[37] M. Vardaro,[42,43] S. Vass,[1] M. Vasúth,[39] R. Vaulin,[11] A. Vecchio,[46] G. Vedovato,[43] J. Veitch,[46] P. J. Veitch,[101] K. Venkateswara,[128] D. Verkindt,[7] F. Vetrano,[58,59] A. Viceré,[58,59] S. Vinciguerra,[46] D. J. Vine,[51] J.-Y. Vinet,[54] S. Vitale,[11] T. Vo,[36] H. Vocca,[33,34] C. Vorvick,[38] W. D. Vousden,[46] S. P. Vyatchanin,[50] A. R. Wade,[21] L. E. Wade,[17] M. Wade,[17] S. J. Waldman,[11] M. Walker,[2] L. Wallace,[1] S. Walsh,[17] G. Wang,[13] H. Wang,[46] M. Wang,[46] X. Wang,[71] Y. Wang,[52] H. Ward,[37] R. L. Ward,[21] J. Warner,[38] M. Was,[7] B. Weaver,[38] L.-W. Wei,[54] M. Weinert,[9] A. J. Weinstein,[1] R. Weiss,[11] T. Welborn,[6] L. Wen,[52] P. Weßels,[9] T. Westphal,[9] K. Wette,[9] J. T. Whelan,[99,9] S. E. Whitcomb,[1] D. J. White,[86] B. F. Whiting,[5] K. Wiesner,[9] C. Wilkinson,[38] P. A. Willems,[1] L. Williams,[5] R. D. Williams,[1] A. R. Williamson,[82] J. L. Willis,[129] B. Willke,[18,9] M. H. Wimmer,[9,18] L. Winkelmann,[9] W. Winkler,[9] C. C. Wipf,[1] A. G. Wiseman,[17] H. Wittel,[9,18] G. Woan,[37] J. Worden,[38] J. L. Wright,[37] G. Wu,[6] J. Yablon,[106] I. Yakushin,[6] W. Yam,[11] H. Yamamoto,[1] C. C. Yancey,[63] M. J. Yap,[21] H. Yu,[11] M. Yvert,[7] A. Zadrożny,[110] L. Zangrando,[43] M. Zanolin,[95] J.-P. Zendri,[43] M. Zevin,[106] F. Zhang,[11] L. Zhang,[1] M. Zhang,[117] Y. Zhang,[99] C. Zhao,[52] M. Zhou,[106] Z. Zhou,[106] X. J. Zhu,[52] M. E. Zucker,[1,11] S. E. Zuraw,[100] and J. Zweizig[1]

[*]Deceased, April 2012. [†]Deceased, May 2015. [‡]Deceased, March 2015.

[§]Present address: National Astronomical Observatory of Japan, 2-21-1 Osawa, Mitaka, Tokyo 181-8588, Japan.

[1]*LIGO, California Institute of Technology, Pasadena, CA 91125, USA*
[2]*Louisiana State University, Baton Rouge, LA 70803, USA*
[3]*Università di Salerno, Fisciano, I-84084 Salerno, Italy*
[4]*INFN, Sezione di Napoli, Complesso Universitario di Monte S.Angelo, I-80126 Napoli, Italy*
[5]*University of Florida, Gainesville, FL 32611, USA*
[6]*LIGO Livingston Observatory, Livingston, LA 70754, USA*
[7]*Laboratoire d'Annecy-le-Vieux de Physique des Particules (LAPP), Université Savoie Mont Blanc, CNRS/IN2P3, F-74941 Annecy-le-Vieux, France*
[8]*University of Sannio at Benevento, I-82100 Benevento, Italy and INFN, Sezione di Napoli, I-80100 Napoli, Italy*
[9]*Albert-Einstein-Institut, Max-Planck-Institut für Gravitationsphysik, D-30167 Hannover, Germany*
[10]*Nikhef, Science Park, 1098 XG Amsterdam, The Netherlands*
[11]*LIGO, Massachusetts Institute of Technology, Cambridge, MA 02139, USA*
[12]*Instituto Nacional de Pesquisas Espaciais, 12227-010 São José dos Campos, SP, Brazil*
[13]*INFN, Gran Sasso Science Institute, I-67100 L'Aquila, Italy*
[14]*INFN, Sezione di Roma Tor Vergata, I-00133 Roma, Italy*
[15]*Inter-University Centre for Astronomy and Astrophysics, Pune 411007, India*
[16]*International Centre for Theoretical Sciences, Tata Institute of Fundamental Research, Bangalore 560012, India*
[17]*University of Wisconsin-Milwaukee, Milwaukee, WI 53201, USA*
[18]*Leibniz Universität Hannover, D-30167 Hannover, Germany*
[19]*Università di Pisa, I-56127 Pisa, Italy*
[20]*INFN, Sezione di Pisa, I-56127 Pisa, Italy*
[21]*Australian National University, Canberra, Australian Capital Territory 0200, Australia*

[22]The University of Mississippi, University, MS 38677, USA
[23]California State University Fullerton, Fullerton, CA 92831, USA
[24]LAL, Univ. Paris-Sud, CNRS/IN2P3, Université Paris-Saclay, Orsay, France
[25]Chennai Mathematical Institute, Chennai, India
[26]Università di Roma Tor Vergata, I-00133 Roma, Italy
[27]University of Southampton, Southampton SO17 1BJ, United Kingdom
[28]Universität Hamburg, D-22761 Hamburg, Germany
[29]INFN, Sezione di Roma, I-00185 Roma, Italy
[30]Albert-Einstein-Institut, Max-Planck-Institut für Gravitationsphysik, D-14476 Potsdam-Golm, Germany
[31]APC, AstroParticule et Cosmologie, Université Paris Diderot, CNRS/IN2P3, CEA/Irfu, Observatoire de Paris, Sorbonne Paris Cité, F-75205 Paris Cedex 13, France
[32]Montana State University, Bozeman, MT 59717, USA
[33]Università di Perugia, I-06123 Perugia, Italy
[34]INFN, Sezione di Perugia, I-06123 Perugia, Italy
[35]European Gravitational Observatory (EGO), I-56021 Cascina, Pisa, Italy
[36]Syracuse University, Syracuse, NY 13244, USA
[37]SUPA, University of Glasgow, Glasgow G12 8QQ, United Kingdom
[38]LIGO Hanford Observatory, Richland, WA 99352, USA
[39]Wigner RCP, RMKI, H-1121 Budapest, Konkoly Thege Miklós út 29-33, Hungary
[40]Columbia University, New York, NY 10027, USA
[41]Stanford University, Stanford, CA 94305, USA
[42]Università di Padova, Dipartimento di Fisica e Astronomia, I-35131 Padova, Italy
[43]INFN, Sezione di Padova, I-35131 Padova, Italy
[44]CAMK-PAN, 00-716 Warsaw, Poland
[45]Astronomical Observatory Warsaw University, 00-478 Warsaw, Poland
[46]University of Birmingham, Birmingham B15 2TT, United Kingdom
[47]Università degli Studi di Genova, I-16146 Genova, Italy
[48]INFN, Sezione di Genova, I-16146 Genova, Italy
[49]RRCAT, Indore MP 452013, India
[50]Faculty of Physics, Lomonosov Moscow State University, Moscow 119991, Russia
[51]SUPA, University of the West of Scotland, Paisley PA1 2BE, United Kingdom
[52]University of Western Australia, Crawley, Western Australia 6009, Australia
[53]Department of Astrophysics/IMAPP, Radboud University Nijmegen, P.O. Box 9010, 6500 GL Nijmegen, The Netherlands
[54]Artemis, Université Cote d'Azur, CNRS, Observatoire Cote d'Azur, CS 34229 , Nice cedex 4, France
[55]MTA Eötvös University, "Lendulet" Astrophysics Research Group, Budapest 1117, Hungary
[56]Institut de Physique de Rennes, CNRS, Université de Rennes 1, F-35042 Rennes, France
[57]Washington State University, Pullman, WA 99164, USA
[58]Università degli Studi di Urbino 'Carlo Bo', I-61029 Urbino, Italy
[59]INFN, Sezione di Firenze, I-50019 Sesto Fiorentino, Firenze, Italy
[60]University of Oregon, Eugene, OR 97403, USA
[61]Laboratoire Kastler Brossel, UPMC-Sorbonne Universités, CNRS, ENS-PSL Research University, Collège de France, F-75005 Paris, France
[62]VU University Amsterdam, 1081 HV Amsterdam, The Netherlands
[63]University of Maryland, College Park, MD 20742, USA
[64]Center for Relativistic Astrophysics and School of Physics, Georgia Institute of Technology, Atlanta, GA 30332, USA
[65]Institut Lumière Matière, Université de Lyon, Université Claude Bernard Lyon 1, UMR CNRS 5306, 69622 Villeurbanne, France
[66]Laboratoire des Matériaux Avancés (LMA), IN2P3/CNRS, Université de Lyon, F-69622 Villeurbanne, Lyon, France
[67]Universitat de les Illes Balears, IAC3—IEEC, E-07122 Palma de Mallorca, Spain
[68]Università di Napoli 'Federico II', Complesso Universitario di Monte S.Angelo, I-80126 Napoli, Italy
[69]NASA/Goddard Space Flight Center, Greenbelt, MD 20771, USA
[70]Canadian Institute for Theoretical Astrophysics, University of Toronto, Toronto, Ontario M5S 3H8, Canada
[71]Tsinghua University, Beijing 100084, China
[72]University of Michigan, Ann Arbor, MI 48109, USA
[73]National Tsing Hua University, Hsinchu City, Taiwan 30013, R.O.C.
[74]Charles Sturt University, Wagga Wagga, New South Wales 2678, Australia
[75]University of Chicago, Chicago, IL 60637, USA
[76]Caltech CaRT, Pasadena, CA 91125, USA
[77]Korea Institute of Science and Technology Information, Daejeon 305-806, Korea

[78]Carleton College, Northfield, MN 55057, USA
[79]Università di Roma 'La Sapienza', I-00185 Roma, Italy
[80]University of Brussels, Brussels 1050, Belgium
[81]Texas Tech University, Lubbock, TX 79409, USA
[82]Cardiff University, Cardiff CF24 3AA, United Kingdom
[83]University of Minnesota, Minneapolis, MN 55455, USA
[84]The University of Melbourne, Parkville, Victoria 3010, Australia
[85]The University of Texas Rio Grande Valley, Brownsville, TX 78520, USA
[86]The University of Sheffield, Sheffield S10 2TN, United Kingdom
[87]Montclair State University, Montclair, NJ 07043, USA
[88]Università di Trento, Dipartimento di Fisica, I-38123 Povo, Trento, Italy
[89]INFN, Trento Institute for Fundamental Physics and Applications, I-38123 Povo, Trento, Italy
[90]The Pennsylvania State University, University Park, PA 16802, USA
[91]School of Mathematics, University of Edinburgh, Edinburgh EH9 3FD, United Kingdom
[92]Indian Institute of Technology, Gandhinagar Ahmedabad Gujarat 382424, India
[93]Institute for Plasma Research, Bhat, Gandhinagar 382428, India
[94]University of Szeged, Dóm tér 9, Szeged 6720, Hungary
[95]Embry-Riddle Aeronautical University, Prescott, AZ 86301, USA
[96]Tata Institute of Fundamental Research, Mumbai 400005, India
[97]Rutherford Appleton Laboratory, HSIC, Chilton, Didcot, Oxon OX11 0QX, United Kingdom
[98]American University, Washington, D.C. 20016, USA
[99]Rochester Institute of Technology, Rochester, NY 14623, USA
[100]University of Massachusetts-Amherst, Amherst, MA 01003, USA
[101]University of Adelaide, Adelaide, South Australia 5005, Australia
[102]West Virginia University, Morgantown, WV 26506, USA
[103]University of Białystok, 15-424 Białystok, Poland
[104]SUPA, University of Strathclyde, Glasgow G1 1XQ, United Kingdom
[105]IISER-TVM, CET Campus, Trivandrum Kerala 695016, India
[106]Northwestern University, Evanston, IL 60208, USA
[107]Institute of Applied Physics, Nizhny Novgorod, 603950, Russia
[108]Pusan National University, Busan 609-735, Korea
[109]Hanyang University, Seoul 133-791, Korea
[110]NCBJ, 05-400 Świerk-Otwock, Poland
[111]IM-PAN, 00-956 Warsaw, Poland
[112]Monash University, Victoria 3800, Australia
[113]Seoul National University, Seoul 151-742, Korea
[114]ESPCI, CNRS, F-75005 Paris, France
[115]Università di Camerino, Dipartimento di Fisica, I-62032 Camerino, Italy
[116]Southern University and A&M College, Baton Rouge, LA 70813, USA
[117]College of William and Mary, Williamsburg, VA 23187, USA
[118]Instituto de Física Teórica, University Estadual Paulista/ICTP South American Institute for Fundamental Research, São Paulo SP 01140-070, Brazil
[119]University of Cambridge, Cambridge CB2 1TN, United Kingdom
[120]IISER-Kolkata, Mohanpur, West Bengal 741252, India
[121]Whitman College, 280 Boyer Ave, Walla Walla, WA 9936, USA
[122]National Institute for Mathematical Sciences, Daejeon 305-390, Korea
[123]Hobart and William Smith Colleges, Geneva, NY 14456, USA
[124]Institute of Astronomy, 65-265 Zielona Góra, Poland
[125]Andrews University, Berrien Springs, MI 49104, USA
[126]Università di Siena, I-53100 Siena, Italy
[127]Trinity University, San Antonio, TX 78212, USA
[128]University of Washington, Seattle, WA 98195, USA
[129]Abilene Christian University, Abilene, TX 79699, USA

On September 14, 2015 at 09:50:45 UTC the two detectors of the Laser Interferometer Gravitational-wave Observatory (LIGO) simultaneously observed a transient gravitational-wave signal. The signal sweeps upwards in frequency from 35 Hz to 250 Hz with a peak gravitational-wave strain of 1.0×10^{-21}. It matches the waveform predicted by general relativity for the inspiral and merger of a pair of black holes and the ringdown of the resulting single black hole. The signal was observed with a matched filter signal-to-noise ratio of 24 and a false alarm rate estimated to be less than 1 event per 200 000 years, equivalent to a significance of greater than $5.1\,\sigma$. The source lies at a luminosity distance of 410^{+160}_{-180} Mpc corresponding to a redshift $z = 0.09^{+0.03}_{-0.04}$. In the source frame, the initial black hole masses are $36^{+5}_{-4}\,\mathrm{M}_\odot$ and $29^{+4}_{-4}\,\mathrm{M}_\odot$, and the final black hole mass is $62^{+4}_{-4}\,\mathrm{M}_\odot$, with $3.0^{+0.5}_{-0.5}\,\mathrm{M}_\odot c^2$ radiated in gravitational waves at a peak luminosity of $3.6^{+0.5}_{-0.4} \times 10^{56}$ erg/s. All uncertainties define 90% credible intervals. These observations demonstrate the existence of binary stellar-mass black hole systems. This is the first direct detection of gravitational waves and the first observation of a binary black hole merger.

PACS numbers: 04.80.Nn, 04.25.dg, 95.85.Sz, 97.80.-d

Introduction — In 1916, the year after the final formulation of the field equations of general relativity, Albert Einstein predicted the existence of gravitational waves. He found that the linearized weak-field equations had wave solutions: transverse waves of spatial strain that travel at the speed of light, generated by time variations of the mass quadrupole moment of the source [1, 2]. Einstein understood that gravitational-wave amplitudes would be remarkably small and expected that they would have no practical importance for physics.

That same year Schwarzschild published a solution for the field equations [3] that was later understood to describe a black hole [4, 5], and in 1963 Kerr generalized the solution to rotating black holes [6]. In the 1970s theoretical work led to the understanding of black hole quasi-normal modes [7–9]. In the past decade, breakthroughs in numerical relativity have produced accurate simulations of binary black hole mergers [10–12]. While numerous black hole candidates have now been identified through electromagnetic observations [13–15], black hole mergers have not previously been observed.

The discovery of the binary pulsar system PSR B1913+16 by Hulse and Taylor [16] and subsequent observations of its energy loss by Taylor and Weisberg [17] demonstrated the existence of gravitational waves. This discovery, along with emerging astrophysical understanding [18], led to the recognition that direct observations of gravitational waves would enable studies of additional relativistic systems and provide new tests of general relativity, especially in the dynamic strong-field regime. Numerical relativity simulations, together with advances in analytical relativity [19, 20], have led to the development of gravitational waveforms for a wide range of such systems.

Prior to the discovery of radio pulsars, experiments to detect gravitational waves began with Weber and his resonant mass detectors in the 1960s [21], followed by an international network of cryogenic resonant detectors [22]. Interferometric detectors were first suggested in the early 1960s [23] and the 1970s [24]. A study of the noise and performance of such detectors [25], and further concepts to improve them [26], led to proposals for long-baseline broadband laser interferometers with the potential for significantly increased sensitivity [27–29]. By 2000 a network of initial detectors had been constructed, including the Laser Interferometer Gravitational-wave Observatory (LIGO) in the United States, GEO 600 in Germany, and Virgo in Italy. This network made joint observations from 2005 through 2011, setting upper limits on a wide variety of gravitational-wave sources. In 2015 Advanced LIGO became the first of a significantly more sensitive network of advanced detectors to begin observations [30–33].

A century after the fundamental predictions of Einstein, Schwarzschild and Kerr, we report the first direct detection of gravitational waves and the first direct observation of a binary black hole system merging to form a single black hole. This confirms general relativity's prediction for the nonlinear dynamics of highly disturbed black holes and provides the first view of general relativity in the strong-field, high-velocity regime.

Observation — On September 14, 2015 at 09:50:45 UTC the LIGO Hanford, WA, and Livingston, LA, observatories detected the coincident signal, referred to as GW150914, shown in Fig. 1 [40]. The initial detection was made by a real-time search for generic gravitational wave transients [41] within three minutes of data acquisition. Subsequently, a matched-filter analysis that uses relativistic models of compact binary waveforms [42] recovered GW150914 as the most significant trigger from each detector. These two triggers occurred within the 10 ms inter-site propagation time and have a combined signal-to-noise ratio (SNR) of 24.

A back-of-the-envelope analysis of the basic features of GW150914 points to it being produced by the coalescence of two black holes – i.e., their orbital inspiral and merger, and subsequent final black hole ringdown. Over 0.2 s, the signal increases in frequency and amplitude in about 8 cycles from 35 to 150 Hz. The most plausible explanation for this evolution is the inspiral of two orbiting masses m_1 and m_2 due to gravitational-wave emission. At the lower frequencies, such evolution is characterized by the chirp

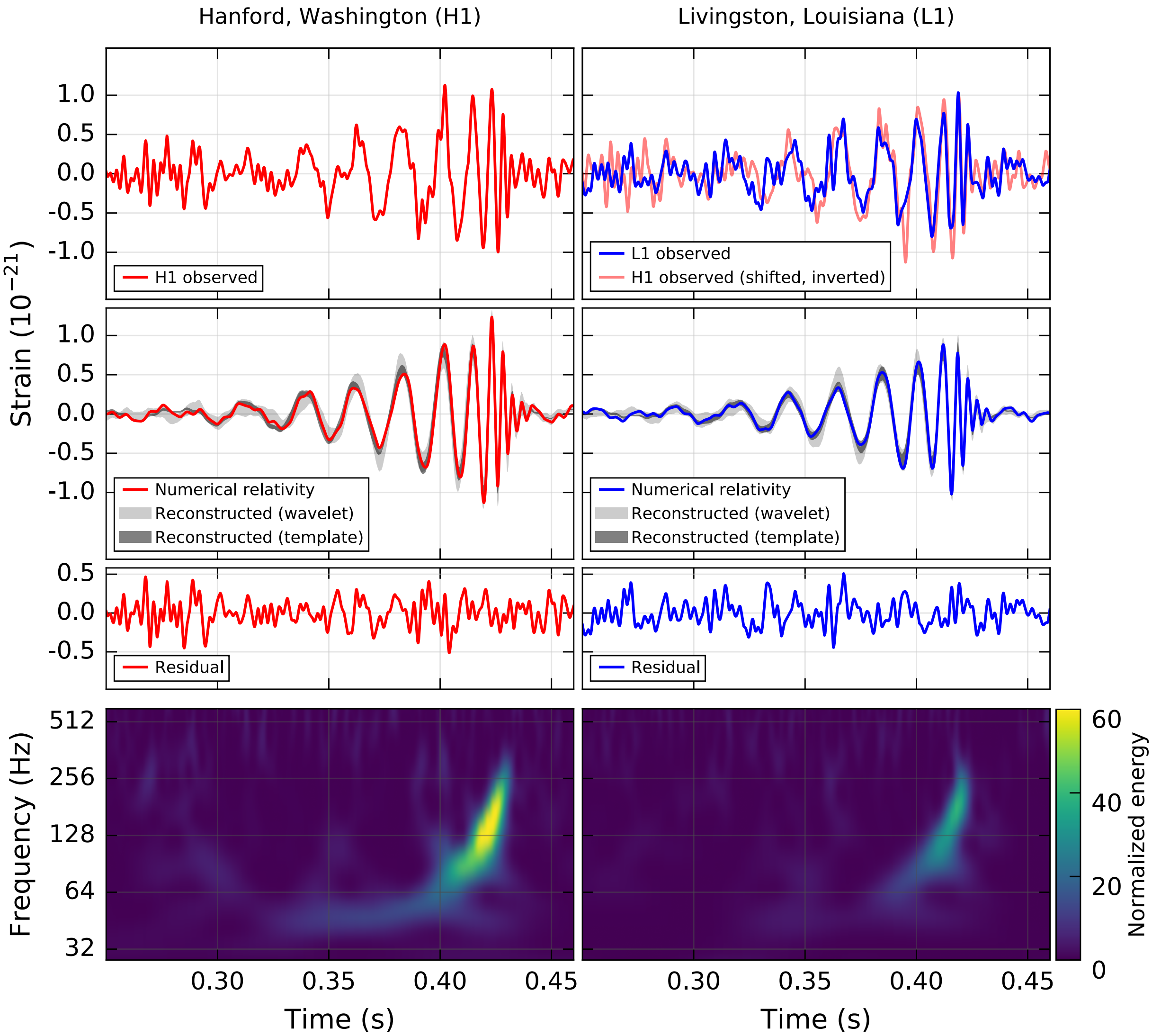

FIG. 1. The gravitational-wave event GW150914 observed by the LIGO Hanford (H1, left column panels) and Livingston (L1, right column panels) detectors. Times are shown relative to September 14, 2015 at 09:50:45 UTC. For visualization, all time series are filtered with a 35–350 Hz band-pass filter to suppress large fluctuations outside the detectors' most sensitive frequency band, and band-reject filters to remove the strong instrumental spectral lines seen in the Fig. 3 spectra. *Top row, left*: H1 strain. *Top row, right*: L1 strain. GW150914 arrived first at L1 and $6.9^{+0.5}_{-0.4}$ ms later at H1; for a visual comparison the H1 data are also shown, shifted in time by this amount and inverted (to account for the detectors' relative orientations). *Second row*: Gravitational-wave strain projected onto each detector in the 35–350 Hz band. Solid lines show a numerical relativity waveform for a system with parameters consistent with those recovered from GW150914 [34, 35] confirmed by an independent calculation based on [11]. Shaded areas show 90% credible regions for two waveform reconstructions: one that models the signal as a set of sine-Gaussian wavelets [36, 37] and one that models the signal using binary-black-hole template waveforms [38]. These reconstructions have a 95% overlap, as shjown in [38]. *Third row*: Residuals after subtracting the filtered numerical relativity waveform from the filtered detector time series. *Bottom row*: A time-frequency decomposition [39] of the signal power associated with GW150914. Both plots show a signal with frequency increasing over time.

mass [43]

$$\mathcal{M} = \frac{(m_1 m_2)^{3/5}}{(m_1+m_2)^{1/5}} = \frac{c^3}{G}\left[\frac{5}{96}\pi^{-8/3} f^{-11/3} \dot{f}\right]^{3/5},$$

where f and $\dot{f}$ are the observed frequency and its time derivative and G and c are the gravitational constant and speed of light. Estimating f and $\dot{f}$ from the Fig. 1 data we obtain a chirp mass of $\mathcal{M} \simeq 30\,\mathrm{M}_\odot$, implying that the total mass $M = m_1 + m_2$ must be at least $\simeq 70\,\mathrm{M}_\odot$. This bounds the sum of the Schwarzschild radii of the binary components to $2GM/c^2 \gtrsim 210\,\mathrm{km}$. To reach the high orbital frequency of 75 Hz (half the gravitational-wave frequency) the objects must have been very close, and hence very compact. (Equal Newtonian point masses orbiting at

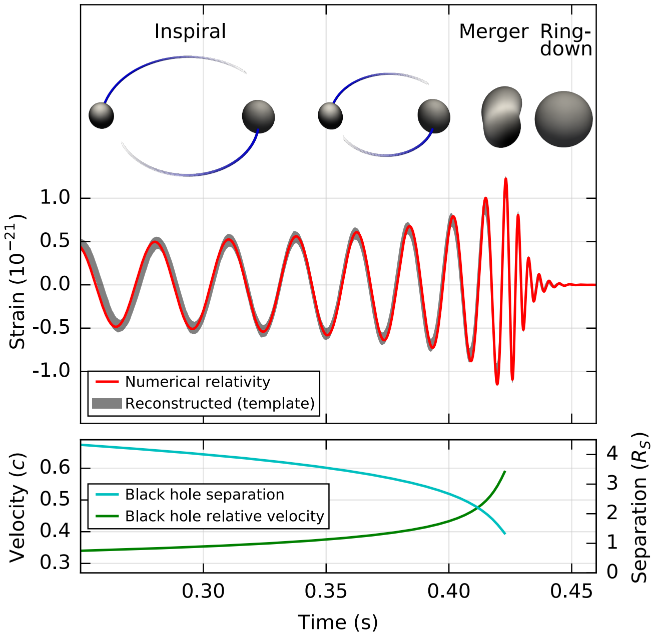

FIG. 2. *Top:* Estimated gravitational-wave strain amplitude from GW150914 projected onto H1. This shows the full bandwidth of the waveforms, without the filtering used for Fig. 1. The inset images show numerical-relativity models of the black-hole horizons as the holes coalesce. *Bottom:* The Keplerian effective black hole separation in units of Schwarzschild radii ($R_S = 2GM/c^2$) and the effective relative velocity given by the Post-Newtonian parameter $v/c = (GM\pi f/c^3)^{1/3}$, where f is the gravitational-wave frequency calculated with numerical relativity and M is the total mass.

this frequency would have been only $\simeq$ 350 km apart.) A pair of neutron stars, while compact, would not have the required mass, while a black hole-neutron star binary with the deduced chirp mass would have a very large total mass, and would thus merge at much lower frequency. This leaves black holes as the only known star types compact enough to reach 75 Hz orbital frequencies without contact. Furthermore, the decay of the waveform after it peaks is consistent with the damped oscillations of a final black hole relaxing to a stationary Kerr configuration. Below, we present a general-relativistic analysis of GW150914; Fig. 2 shows the calculated waveform using the resulting source parameters.

Detectors — Gravitational-wave astronomy exploits multiple, widely separated detectors to distinguish gravitational waves from local instrumental and environmental noise, to provide source sky localization from relative arrival times, and to measure wave polarizations. The LIGO sites each operate a single Advanced LIGO detector [30], a modified Michelson interferometer that measures gravitational-wave strain as a difference in length of its orthogonal arms. Each arm is formed by two mirrors, acting as test masses, separated by $L_x = L_y = L = 4$ km, as shown in Fig. 3. A passing gravitational wave effectively alters the arm lengths such that the measured difference is $\Delta L(t) = L_x - L_y = h(t)L$, where h is the gravitational-wave strain amplitude projected onto the detector. This differential length variation alters the phase difference between the two light fields returning to the beamsplitter, transmitting an optical signal proportional to the gravitational-wave strain to the output photodetector, as shown in Fig. 3.

To achieve sufficient sensitivity to measure gravitational waves the detectors include several enhancements to the basic Michelson interferometer. First, each arm contains a resonant optical cavity, formed by its two test mass mirrors, that multiplies the effect of a gravitational wave on the light phase by a factor of 300 [45]. Second, a partially transmissive power-recycling mirror at the input provides additional resonant buildup of the laser light in the interferometer as a whole [46, 47]: 20 W of laser input is increased to 700 W incident on the beamsplitter, which is further increased to 100 kW circulating in each arm cavity. Third, a partially transmissive signal-recycling mirror at the output optimizes the gravitational-wave signal extraction by broadening the bandwidth of the arm cavities [48, 49]. The interferometer is illuminated with a 1064-nm wavelength Nd:YAG laser, stabilized in amplitude, frequency, and beam geometry [50, 51]. The gravitational-wave signal is extracted at the output port using homodyne readout [52].

These interferometry techniques are designed to maximize the conversion of strain to optical signal, thereby minimizing the impact of photon shot noise (the principal noise at high frequencies). High strain sensitivity also requires that the test masses have low displacement noise, which is achieved by isolating them from seismic noise (low frequencies) and designing them to have low thermal noise (mid frequencies). Each test mass is suspended as the final stage of a quadruple pendulum system [53], supported by an active seismic isolation platform [54]. These systems collectively provide more than 10 orders of magnitude of isolation from ground motion for frequencies above 10 Hz. Thermal noise is minimized by using low-mechanical-loss materials in the test masses and their suspensions: the test masses are 40-kg fused silica substrates with low-loss dielectric optical coatings [55], and are suspended with fused silica fibers from the stage above [56].

To minimize additional noise sources, all components other than the laser source are mounted on vibration isolation stages in ultra-high vacuum. To reduce optical phase fluctuations caused by Rayleigh scattering, the pressure in the 1.2-m diameter tubes containing the arm-cavity beams is maintained below 1 μPa.

Servo controls are used to hold the arm cavities on resonance [57] and maintain proper alignment of the optical components [58]. The detector output is calibrated in strain by measuring its response to test mass motion induced by photon pressure from a modulated calibration laser beam [59]. The calibration is established to an un-

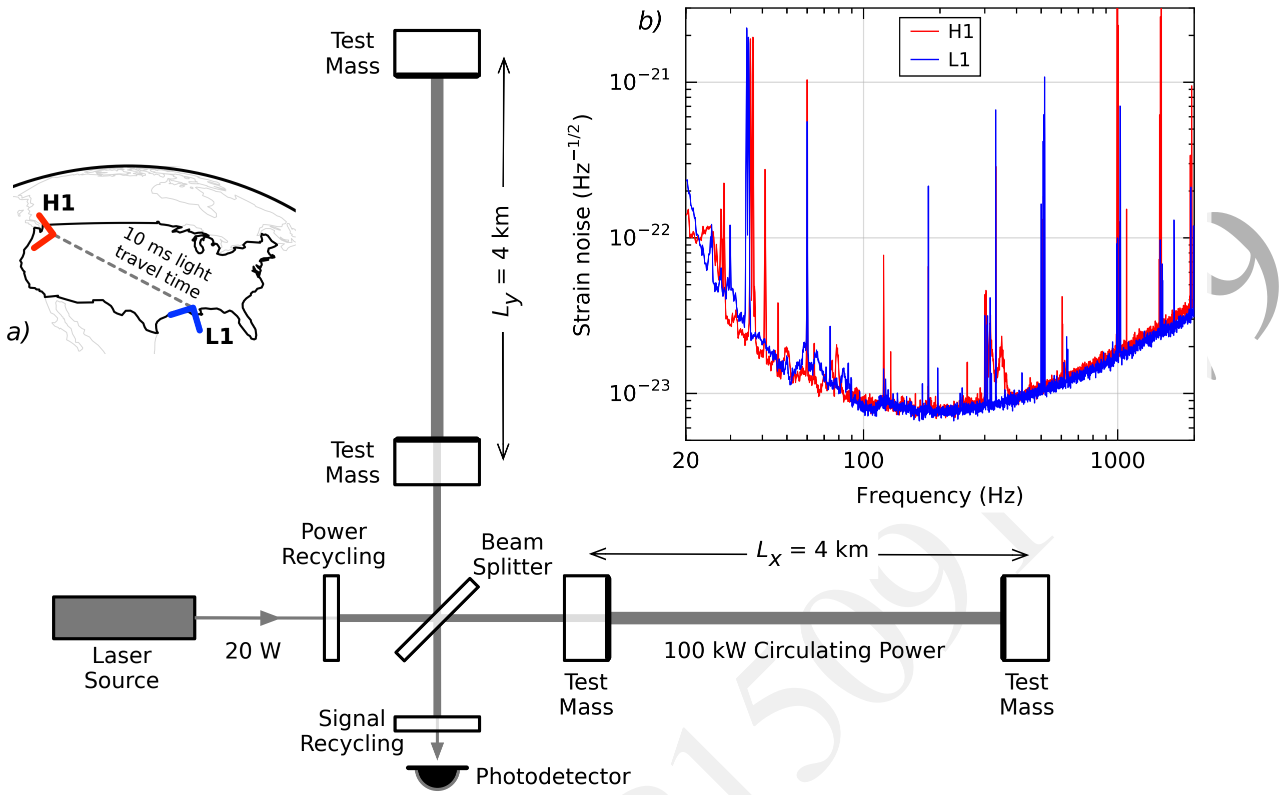

FIG. 3. Simplified diagram of an Advanced LIGO detector (not to scale). A gravitational wave propagating orthogonally to the detector plane and linearly polarized parallel to the 4-km optical cavities will have the effect of lengthening one 4-km arm and shortening the other during one half-cycle of the wave; these length changes are reversed during the other half-cycle. The output photodetector records these differential cavity length variations. While a detector's directional response is maximal for this case, it is still significant for most other angles of incidence or polarizations (gravitational waves propagate freely through the Earth). Inset *a*: Location and orientation of the LIGO detectors at Hanford, WA (H1) and Livingston, LA (L1). Inset *b*: The instrument noise for each detector near the time of the signal detection; this is an amplitude spectral density, expressed in terms of equivalent gravitational-wave strain amplitude. The sensitivity is limited by photon shot noise at frequencies above 150 Hz, and by a superposition of technical noise sources at lower frequencies [44]. Narrowband features include calibration lines (33 – 38 Hz, 330 Hz, and 1080 Hz), vibrational modes of suspension fibers (500 Hz and harmonics), and 60 Hz electric power grid harmonics.

certainty of less than 10% in amplitude and 10 degrees in phase, and is continuously monitored with calibration laser excitations at selected frequencies. Two alternative methods are used to validate the absolute calibration, one referenced to the main laser wavelength and the other to a radio-frequency oscillator [60]. Additionally, the detector response to gravitational waves is tested by injecting simulated waveforms with the calibration laser.

To monitor environmental disturbances and their influence on the detectors, each observatory site is equipped with an array of sensors: seismometers, accelerometers, microphones, magnetometers, radio receivers, weather sensors, AC-power line monitors, and a cosmic-ray detector [61]. Another $\sim 10^5$ channels record the interferometer's operating point and the state of the control systems. Data collection is synchronized to Global Positioning System (GPS) time to better than 10 μs [62]. Timing accuracy is verified with an atomic clock and a secondary GPS receiver at each observatory site.

In their most sensitive band, 100 – 300 Hz, the current LIGO detectors are 3 to 5 times more sensitive to strain than initial LIGO [63]; at lower frequencies, the improvement is even greater, with more than ten times better sensitivity below 60 Hz. Because the detectors respond proportionally to gravitational-wave amplitude, for small redshifts the volume of space to which they are sensitive increases as the cube of strain sensitivity. For binary black holes with masses similar to GW150914, the space-time volume surveyed by the observations reported here surpasses previous observations by an order of magnitude [64].

Detector Validation — Exhaustive investigations of instrumental and environmental disturbances were performed, giving no evidence to suggest that GW150914 could be an instrumental artifact [65]. The detectors' susceptibility to environmental disturbances was quantified by measuring their response to specially generated magnetic, radio frequency, acoustic, and vibration excitations. These tests indicated that any external disturbance large enough to have caused the observed signal would have been clearly recorded by the array of environmental sensors. None of the environmental sensors recorded any disturbances that evolved in time and frequency like GW150914, and all environmental fluctuations during the second that contained GW150914 were at least 17 times too small to account for its amplitude. Special care was taken to search for any possible long-range correlated disturbances which might produce near simultaneous signals at the two sites; none were found.

The detector strain data exhibit non-Gaussian noise transients that arise from a variety of instrumental mechanisms. Many have distinct signatures, visible in auxiliary data channels that are not sensitive to gravitational waves; such instrumental transients are removed from our analyses. Any instrumental transients that remain in the data are accounted for in the estimated detector backgrounds described below. There is no evidence for instrumental transients that are temporally correlated between the two detectors.

Searches — We present the analysis of 16 d of coincident observations between the two LIGO detectors from September 12 to October 20. This is a subset of the data from Advanced LIGO's first observational period that ended on January 12, 2016.

GW150914 is confidently detected by two different types of searches. One aims at recovering signals from the coalescence of compact objects, using optimal matched filtering with waveforms predicted by general relativity. The other search targets a broad range of generic transient signals, with minimal assumptions about waveforms. These searches use independent methods and their response to detector noise consists of different, uncorrelated, events. However, strong signals from binary black hole mergers are expected to be detected by both searches.

Each search identifies candidate events that are detected at both observatories consistent with the inter-site propagation time. They are assigned a detection-statistic value that ranks their signal likelihood. The significance of a candidate event is determined by the search background – the rate at which detector noise produces events with a detection-statistic value equal to or higher than the candidate event. Estimating this background is challenging for two reasons: the detector noise is non-stationary and non-Gaussian, so its properties must be empirically determined; and it is not possible to shield the detector from gravitational waves to directly measure a signal-free background. Though the specific procedure used to estimate the background is slightly different for the two searches, both use a time-shift technique: the timestamps of one detector's data are artificially shifted by an offset that is large compared to the inter-site propagation time, and a new set of events is produced based on this time-shifted data set. For instrumental noise that is uncorrelated between detectors this is an effective way to estimate the background. In this process a gravitational-wave signal in one detector may coincide with time-shifted noise transients in the other detector, thereby contributing to the background estimate. This leads to an overestimate of the noise background and therefore to a more conservative assessment of the significance of candidate events.

Non-Gaussian detector noise occurs in different time-frequency regions. This means that the search background is not uniform across the parameter space being searched. To maximize sensitivity and provide a better estimate of event significance, the searches sort both their background estimates and their event candidates into different classes according to their time-frequency morphology. The significance of a candidate event is measured against the background of its class. To account for having searched multiple classes, this significance is decreased by a trials factor equal to the number of classes [66].

Generic-transients search — Designed to operate without a specific waveform model, this search identifies coincident excess power in time-frequency representations of the detector strain data [41, 67], for signal frequencies up to 1 kHz and durations up to a few seconds.

Using a multi-detector maximum likelihood method, this search reconstructs signal waveforms consistent with a common gravitational wave signal in both detectors. Each event is ranked according to the detection-statistic $\eta_c = \sqrt{2E_c/(1 + E_n/E_c)}$, where E_c is the dimensionless coherent signal energy obtained by cross-correlating the two reconstructed waveforms, and E_n is the dimensionless residual noise energy after the reconstructed signal is subtracted from the data. The statistic η_c thus quantifies the consistency of the data between the two detectors.

Based on their time-frequency morphology, the events are divided into three mutually exclusive search classes, as described in [37]: events with frequency increasing with time and not similar to known populations of noise transients (class C3), events not similar to populations of noise transients but whose frequency does not increase with time (class C2), and the remaining events (class C1).

Detected with $\eta_c = 20.0$, GW150914 is the strongest event of the entire search. Consistently with its coalescence signal signature it is found in the search class C3 of events with increasing time-frequency evolution. Measured on a background equivalent to over 67 400 years of data and including a trials factor of 3 to account for the search classes, its false alarm rate is lower than 1 in 22 500 years. This corresponds to a probability $< 2 \times 10^{-6}$ of observing at least one noise event during the analysis time as strong as GW150914, equivalent to 4.6 σ.

The selection criteria that defines the search class C3 where GW150914 was found reduces the background by

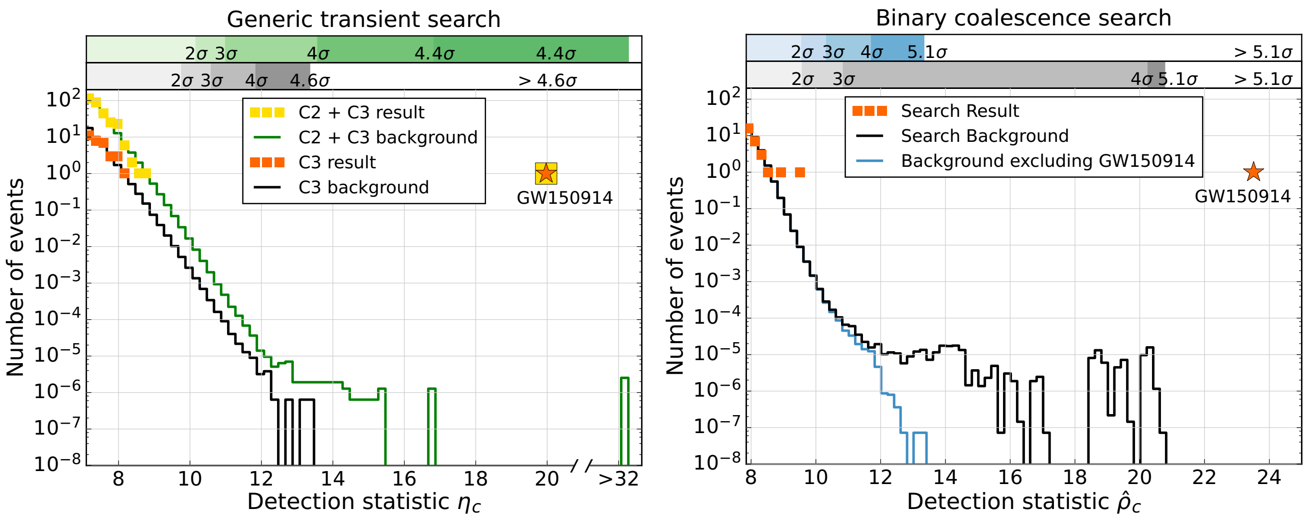

FIG. 4. The search results from the generic-transients search (left) and the binary coalescence search (right). These histograms show the number of candidate events (orange markers) and the number of background events in the search class where GW150914 was found (black lines) as a function of the search detection-statistic and with a bin width of 0.2. The significance of GW150914 is greater than 5.1 σ and 4.6 σ for the binary coalescence and the generic-transients searches, respectively. In the left panel we also show the results (markers in yellow) and the background (green curve) for the search class where GW150914 was found in a generic-transients search with no increasing frequency class (no C3 class). As explained in the text, in this search the GW150914 search class is the C2+C3 class. The tail in the black-line background of the binary coalescence search is due to random coincidences of GW150914 in one detector with noise in the other detector. (This type of event is practically absent in the generic-transients search background because they do not pass the time-frequency consistency requirements used in that search.) The blue curve is the background excluding coincidences involving GW150914 and it is the background to be used to assess the significance of the second strongest event. The scales immediately above the histogram give the significance of an event based on the corresponding color noise backgrounds in Gaussian standard deviations as a function of the detection-statistic.

introducing a constraint on the signal morphology. In order to illustrate the significance of GW150914 against a background of events consistent in both detectors but with arbitrary shapes, we present the results of a search comprising only the two search classes C1 and C2+C3. This is a search that does not have a specific class for events with increasing frequency. As expected, GW150914 is found in the C2+C3 class. In the background of this class there are four events with $\eta_c \geq 32.1$, yielding a false alarm rate for GW150914 of 1 in 8 400 years. This corresponds to a false alarm probability of 5×10^{-6} equivalent to 4.4 σ.

For robustness and validation, we also use other generic-transient search algorithms [37]. A different search [68] and a parameter estimation follow-up [69] detected GW150914 with consistent significance and signal parameters.

Binary coalescence search — This search targets gravitational-wave emission from binary systems with individual masses from 1 $M_\odot$ to 99 $M_\odot$ with total mass less than 100 $M_\odot$ and dimensionless spins up to 0.99 [70]. To model such systems, we use the effective-one-body (EOB) formalism [71], which combines results from the Post-Newtonian approach [72, 73] with results from black hole perturbation theory and numerical relativity. The waveform model [74, 75] assumes that the spins of the merging objects are aligned with the orbital angular momentum, but the resulting templates can nonetheless effectively recover systems with misaligned spins in the parameter region of GW150914 [70]. Approximately 250,000 template waveforms are used to cover this parameter space.

The search calculates the matched-filter signal-to-noise ratio $\rho(t)$ for each template in each detector, and identifies maxima of $\rho(t)$ with respect to the time of arrival of the signal [76–78]. For each maximum we calculate a chi-squared statistic χ_r^2 to test whether the data in several different frequency bands are consistent with the matching template [79]. Values of χ_r^2 near unity indicate that the signal is consistent with a coalescence. If χ_r^2 is greater than unity, $\rho(t)$ is re-weighted as $\hat{\rho} = \rho/[(1 + (\chi_r^2)^3)/2]^{1/6}$ [80, 81]. The final step enforces coincidence between detectors by selecting event pairs that occur within a 15 ms window and have the same matching template. The 15 ms window is determined by the maximum travel time between detectors and uncertainty in the measurement of the arrival time. We rank coincident events based on the quadrature sum $\hat{\rho}_c$ of the $\hat{\rho}$ from both detectors [42].

To produce background data for this search the SNR maxima of one detector are time-shifted by a multiple of 0.1 s and a new set of coincident events is computed. Re-

TABLE I. Estimated source parameters for GW150914. We report the median value as well as the range of the 90% credible interval. Masses are measured in the source frame; to convert masses to detector frame, multiply by $(1+z)$ [84]. The source redshift assumes standard cosmology [85].

Primary black hole mass	$36^{+5}_{-4}\,\mathrm{M}_\odot$
Secondary black hole mass	$29^{+4}_{-4}\,\mathrm{M}_\odot$
Final black hole mass	$62^{+4}_{-4}\,\mathrm{M}_\odot$
Final black hole spin	$0.67^{+0.05}_{-0.07}$
Luminosity distance	410^{+160}_{-180} Mpc
Source redshift, z	$0.09^{+0.03}_{-0.04}$

peating this procedure 1.4×10^7 times produces a noise background analysis time equivalent to 607 800 years. More time slides could be afforded for this search compared to the generic transients search because the time-shift analysis of the latter is more computationally intensive.

To account for the search background noise varying across the target signal space, candidate and background events are divided into three search-classes based on template length. The right panel of Fig. 4 shows the background for the search class of GW150914. The GW150914 detection-statistic value of $\hat{\rho}_c = 23.6$ is larger than any background event, so only an upper bound can be placed on its false alarm rate. Across the three search classes this bound is 1 in 200 000 yrs. This translates to a false alarm probability $< 2 \times 10^{-7}$, corresponding to $5.1\,\sigma$.

A second, independent matched-filter analysis that uses a different method for estimating the significance of its events [82, 83], also detected GW150914 with identical signal parameters and consistent significance.

When an event is confidently identified as a real gravitational wave signal, as for GW150914, the background used to determine the significance of other events is re-estimated without the contribution of this event. This is the background distribution shown as a blue line in the right panel of Fig. 4. Based on this, the second most significant event has a false alarm rate of 1 per 2.3 years and corresponding Poissonian false alarm probability of 0.02.

Source Discussion — The matched filter search is optimized for detecting signals, but it provides only approximate estimates of the source parameters. To refine them, we use the most accurate, general relativity-based models available [74, 75, 86, 87], and perform a coherent Bayesian analysis of the data to derive posterior distributions of the source parameters [88]. These results are summarized in Table I and discussed in detail in [38]. The binary's orbital plane is only loosely constrained, with the total angular momentum most likely being roughly anti-aligned to the line of sight. With the loose constraint on the orbital orientation, and the short duration of the signal in the detectors sensitive band, only weak constraints can be placed on the spins of the binary components; less than 0.7 and 0.9 at 90% confidence for the primary and secondary black hole, respectively. Numerical simulations of binary black-hole mergers provide estimates of the final mass and spin of the merger product, as well as the total energy radiated in gravitational waves and the peak gravitational-wave luminosity. We estimate the total energy radiated in gravitational waves was $3.0^{+0.5}_{-0.5}\,\mathrm{M}_\odot c^2$, where error bars incorporate both measurement uncertainty on the component masses and spins, and systematic uncertainty in fits to numerical simulations [89]. The system reached a peak luminosity of $3.6^{+0.5}_{-0.4} \times 10^{56}$ erg/s equivalent to $200^{+30}_{-20}\,\mathrm{M}_\odot c^2/\mathrm{s}$. This is the most energetic astronomical event ever observed.

Several analyses have been performed to determine whether GW150914 is consistent with a binary black hole in general relativity [90]. A first consistency check involves the mass and spin of the final black hole. In general relativity, the end product of a black hole binary coalescence is a Kerr black hole, which is fully described by its mass and spin. For quasicircular inspirals, these are predicted uniquely by Einstein's equations as a function of the masses and spins of the two progenitor black holes. Using fitting formulae calibrated to numerical relativity simulations [89], we verified that the remnant mass and spin deduced from the early stage of the coalescence and those inferred independently from the late stage are consistent with each other, with no evidence for disagreement from general relativity.

Within the Post-Newtonian formalism, the phase of the gravitational waveform during the inspiral can be expressed as a power-series in the $f^{1/3}$. The coefficients of this expansion can be computed in general relativity. So we can test for consistency with general relativity [91, 92] by allowing their values to deviate from the nominal values, and seeing if the resulting waveform is consistent with the data. In a second check [90] we place constraints on these deviations, finding no evidence for violations of general relativity.

Finally, assuming a modified dispersion relation for gravitational waves, the Compton wavelength of the graviton is constrained to be $\lambda_g > 10^{13}\,\mathrm{km}$ which corresponds to a bound on the graviton mass $m_g < 1.2 \times 10^{-22}\,\mathrm{eV/c^2}$. This improves on Solar System and binary pulsar bounds [93–95] by one and three orders of magnitude, respectively, but does not improve the model-dependent bounds derived from dynamics of galaxy clusters [96] and weak lensing observations [97]. In summary, all three tests are consistent with the predictions of general relativity in the strong-field regime of gravity.

GW150914 demonstrates the existence of stellar-mass black holes more massive than $\gtrsim 25\,\mathrm{M}_\odot$, and establishes that binary black holes can form in Nature and merge within a Hubble time. Binary black holes have been predicted to form both in isolated binaries [98–100] and in dense environments by dynamical interactions [101–103].

Formation of such massive black holes from stellar evolution requires weak massive-star winds, which are possible in stellar environments with metallicity lower than $\simeq 1/2$ the solar value [104, 105]. Further astrophysical implications of this binary black hole discovery are discussed in [106].

By combining our observational results with an estimate of the detection sensitivity for binary black hole mergers, we can constrain the rate of stellar-mass binary black hole mergers in the local universe. An optimally oriented, optimally located binary system otherwise like GW150914 will produce a SNR of 8 in a single detector with sensitivity like those shown in Fig. 3 at luminosity distance 2.4 Gpc ($z = 0.42$). Assuming that all binary black holes in the universe have the same masses and spins as GW150914 [107] and adopting a false alarm rate threshold of 1 per 100 years, we then infer a 90% credible range for the rate of $2 - 53\,\mathrm{Gpc}^{-3}\mathrm{yr}^{-1}$ (in the comoving frame). When we incorporate the full set of binary coalescence search results, properly accounting for each event's probability of astrophysical or terrestrial origin [108], and make more reasonable assumptions about the mass distribution [109], we obtain a higher rate estimate ranging from $6 - 400\,\mathrm{Gpc}^{-3}\mathrm{yr}^{-1}$. These estimates are consistent with the broad range of rate predictions as reviewed in [109], with only the low end ($<1\,\mathrm{Gpc}^{-3}\mathrm{yr}^{-1}$) of rate predictions being excluded.

Binary black hole systems at larger distances contribute to a stochastic background of gravitational waves from the superposition of unresolved systems. Predictions for such a background are presented in [110], and, if the signal from such a population is detected, it would provide information into the evolution of such binary systems over the history of the universe.

Conclusion — The LIGO detectors have observed gravitational waves from the merger of two stellar-mass black holes. The detected waveform matches the predictions of general relativity for the inspiral and merger of a pair of black holes and the ringdown of the resulting single black hole. These observations demonstrate the existence of binary stellar-mass black hole systems. This is the first direct detection of gravitational waves and the first observation of a binary black hole merger.

Efforts are underway to significantly enhance the global gravitational wave detector network [111]. These include further commissioning of the Advanced LIGO detectors to reach design sensitivity, which will allow detection of binaries like GW150914 with 3 times higher SNR. Additionally, Advanced Virgo, KAGRA, and a possible third LIGO detection in India [112] will extend the network and significantly improve the position reconstruction and parameter estimation of sources.

Further details about these results and associated data releases are available at `http://losc.ligo.org/events/GW150914`.

Acknowledgments — The authors gratefully acknowledge the support of the United States National Science Foundation (NSF) for the construction and operation of the LIGO Laboratory and Advanced LIGO as well as the Science and Technology Facilities Council (STFC) of the United Kingdom, the Max-Planck-Society (MPS), and the State of Niedersachsen/Germany for support of the construction of Advanced LIGO and construction and operation of the GEO600 detector. Additional support for Advanced LIGO was provided by the Australian Research Council. The authors gratefully acknowledge the Italian Istituto Nazionale di Fisica Nucleare (INFN), the French Centre National de la Recherche Scientifique (CNRS) and the Foundation for Fundamental Research on Matter supported by the Netherlands Organisation for Scientific Research, for the construction and operation of the Virgo detector and the creation and support of the EGO consortium. The authors also gratefully acknowledge research support from these agencies as well as by the Council of Scientific and Industrial Research of India, Department of Science and Technology, India, Science & Engineering Research Board (SERB), India, Ministry of Human Resource Development, India, the Spanish Ministerio de Economía y Competitividad, the Conselleria d'Economia i Competitivitat and Conselleria d'Educació, Cultura i Universitats of the Govern de les Illes Balears, the National Science Centre of Poland, the FOCUS Programme of Foundation for Polish Science, the European Commission, the Royal Society, the Scottish Funding Council, the Scottish Universities Physics Alliance, the Lyon Institute of Origins (LIO), the National Research Foundation of Korea, Industry Canada and the Province of Ontario through the Ministry of Economic Development and Innovation, the National Science and Engineering Research Council Canada, the Brazilian Ministry of Science, Technology, and Innovation, the Research Corporation, Ministry of Science and Technology (MOST), Taiwan and the Kavli Foundation. The authors gratefully acknowledge the support of the NSF, STFC, MPS, INFN, CNRS and the State of Niedersachsen/Germany for provision of computational resources.

[1] A. Einstein, Sitzungsberichte der Königlich Preußischen Akademie der Wissenschaften (Berlin) **1**, 688 (1916).
[2] A. Einstein, Sitzungsberichte der Königlich Preußischen Akademie der Wissenschaften (Berlin) **1**, 154 (1918).
[3] K. Schwarzschild, Sitzungsberichte der Königlich Preußischen Akademie der Wissenschaften (Berlin) **1**, 189 (1916).
[4] D. Finkelstein, Phys. Rev. **110**, 965 (1958).
[5] M. D. Kruskal, Phys. Rev. **119**, 1743 (1960).
[6] R. P. Kerr, Phys. Rev. Lett. **11**, 237 (1963).
[7] C. V. Vishveshwara, Nature **227**, 936 (1970).
[8] W. H. Press, Astrophys. J. **170**, L105 (1971).
[9] S. Chandrasekhar and S. L. Detweiler, Proc. Roy. Soc. Lond. **A344**, 441 (1975).

[10] F. Pretorius, Phys. Rev. Lett. **95**, 121101 (2005), arXiv:gr-qc/0507014 [gr-qc].

[11] M. Campanelli, C. O. Lousto, P. Marronetti, and Y. Zlochower, Phys. Rev. Lett. **96**, 111101 (2006), arXiv:0511048 [gr-qc].

[12] J. G. Baker, J. Centrella, D.-I. Choi, M. Koppitz, and J. van Meter, Phys. Rev. Lett. **96**, 111102 (2006), arXiv:gr-qc/0511103 [gr-qc].

[13] B. L. Webster and P. Murdin, Nature **235**, 37 (1972).

[14] C. T. Bolton, Nature **240**, 124 (1972).

[15] J. Casares and P. G. Jonker, Space Sci. Rev. **183**, 223 (2014), arXiv:1311.5118 [astro-ph.HE].

[16] R. A. Hulse and J. H. Taylor, Astrophys. J. **195**, L51 (1975).

[17] J. H. Taylor and J. M. Weisberg, Astrophys. J. **253**, 908 (1982).

[18] W. Press and K. Thorne, Annu. Rev. Astron. Astrophys. **10**, 335 (1972).

[19] L. Blanchet, Living Rev. Rel. **17**, 2 (2014), arXiv:1310.1528 [gr-qc].

[20] A. Buonanno and T. Damour, Phys. Rev. D **59**, 084006 (1999), arXiv:gr-qc/9811091 [gr-qc].

[21] J. Weber, Phys. Rev. **117**, 306 (1960).

[22] P. Astone *et al.*, Phys. Rev. D **82** (2010).

[23] M. E. Gertsenshtein and V. I. Pustovoit, Sov. Phys. – JETP **16**, 433 (1962).

[24] G. E. Moss, L. R. Miller, and R. L. Forward, Appl. Opt. **10**, 2495 (1971).

[25] R. Weiss, *Electromagnetically coupled broadband gravitational antenna*, Tech. Rep. (MIT, 1972) Quarterly report of the Research Laboratory for Electronics. https://dcc.ligo.org/LIGO-P720002/public.

[26] R. W. P. Drever, in *Gravitational Radiation*, edited by N. Deruelle and T. Piran (North-Holland, Amsterdam, 1983) p. 321.

[27] A. Abramovici *et al.*, Science **256**, 325 (1992).

[28] A. Brillet, A. Giazotto, *et al.*, *The Virgo Project*, Tech. Rep. VIR-0517A-15 (Virgo Collaboration, 1989) https://tds.ego-gw.it/ql/?c=11247.

[29] J. Hough *et al.*, *Proposal for a Joint German-British Interferometric Gravitational Wave Detector*, Tech. Rep. 147 (MPQ Report, 1989) GWD/137/JH(89). http://eprints.gla.ac.uk/114852.

[30] J. Aasi *et al.*, Class. Quantum Grav. **32**, 074001 (2015), arXiv:1411.4547 [gr-qc].

[31] F. Acernese *et al.*, Class. Quantum Grav. **32**, 024001 (2015), arXiv:1408.3978 [gr-qc].

[32] C. Affeldt *et al.*, Class. Quantum Grav. **31**, 224002 (2014).

[33] Y. Aso *et al.*, Phys. Rev. D **88**, 043007 (2013), arXiv:1306.6747 [gr-qc].

[34] Waveform shown is SXS:BBH:0305 available for download at http://www.black-holes.org/waveforms.

[35] A. H. Mroué *et al.*, Phys. Rev. Lett. **111**, 241104 (2013).

[36] N. J. Cornish and T. B. Littenberg, Class. Quantum Grav. **32**, 135012 (2015), arXiv:1410.3835 [gr-qc].

[37] B. Abbott *et al.*, (2016), https://dcc.ligo.org/LIGO-P1500229/public.

[38] B. Abbott *et al.*, (2016), https://dcc.ligo.org/LIGO-P1500218/public.

[39] S. Chatterji *et al.*, Class. Quantum Grav. **21**, S1809 (2004).

[40] Only the LIGO detectors were collecting data at this time. The Virgo detector was being upgraded to Advanced Virgo, and the GEO detector was in operation but not in observational mode on the day of the event.

[41] S. Klimenko *et al.*, "Method for Detection and reconstruction of gravitational wave transients with networks of advanced detectors," (2015), arXiv:1511.05999 [gr-qc].

[42] S. A. Usman *et al.*, "An improved pipeline to search for gravitational waves from compact binary coalescence," (2015), arXiv:1508.02357 [gr-qc].

[43] P. C. Peters, Phys. Rev. **136**, B1224 (1964).

[44] B. Abbott *et al.*, (2016), https://dcc.ligo.org/LIGO-P1500237/public.

[45] R. W. P. Drever, *The Detection of Gravitational Waves*, edited by D. G. Blair (Cambridge University Press, 1991).

[46] R. W. P. Drever *et al.*, in *Quantum Optics, Experimental Gravity, and Measurement Theory*, NATO ASI Series B, Vol. 94, edited by P. Meystre and M. O. Scully (Plenum Press, New York, 1983) pp. 503–514.

[47] R. Schilling, unpublished (1983).

[48] B. J. Meers, Phys. Rev. D **38**, 2317 (1988).

[49] J. Mizuno *et al.*, Phys. Lett. A **175**, 273 (1993).

[50] P. Kwee *et al.*, Opt. Express **20**, 10617 (2012).

[51] C. L. Mueller *et al.*, To be published in Review of Scientific Instruments (2015).

[52] T. T. Fricke *et al.*, Class. Quantum Grav. **29**, 065005 (2012).

[53] S. M. Aston *et al.*, Class. Quantum Grav. **29**, 235004 (2012).

[54] F. Matichard *et al.*, Class. Quantum Grav. **32**, 185003 (2015).

[55] G. M. Harry *et al.*, Class. Quantum Grav. **24**, 405 (2007), arXiv:0610004 [gr-qc].

[56] A. V. Cumming *et al.*, Class. Quantum Grav. **29**, 035003 (2012).

[57] A. Staley *et al.*, Class. Quantum Grav. **31**, 245010 (2014).

[58] L. Barsotti, M. Evans, and P. Fritschel, Class. Quantum Grav. **27**, 084026 (2010).

[59] B. Abbott *et al.*, (2016), https://dcc.ligo.org/LIGO-P1500248/public.

[60] E. Goetz *et al.*, *Gravitational waves. Proceedings, 8th Edoardo Amaldi Conference, Amaldi 8, New York, USA, June 22-26, 2009*, Class. Quantum Grav. **27**, 084024 (2010), arXiv:0911.0853 [gr-qc].

[61] A. Effler *et al.*, Class. Quantum Grav. **32**, 035017 (2015), arXiv:1409.5160 [astro-ph.IM].

[62] I. Bartos *et al.*, Class. Quantum Grav. **27**, 084025 (2010).

[63] J. Aasi *et al.*, Class. Quantum Grav. **32**, 115012 (2015), arXiv:1410.7764 [gr-qc].

[64] J. Aasi *et al.*, Phys. Rev. D **87**, 022002 (2013), arXiv:1209.6533 [gr-qc].

[65] B. Abbott *et al.*, (2016), https://dcc.ligo.org/LIGO-P1500227/public.

[66] L. Lyons, Ann. Appl. Stat. **2**, 887 (2008).

[67] S. Klimenko *et al.*, Class. Quantum Grav. **25**, 114029 (2008).

[68] R. Lynch *et al.*, "An information-theoretic approach to the gravitational wave burst detection problem," (2015), arXiv:1511.05955 [gr-qc].

[69] J. Kanner *et al.*, "Leveraging waveform complexity for confident detection of gravitational waves," (2015),

arXiv:1509.06423.

[70] B. Abbott *et al.*, (2016), `https://dcc.ligo.org/LIGO-P1500269/public`.

[71] A. Buonanno and T. Damour, Phys. Rev. D **62**, 064015 (2000), arXiv:gr-qc/0001013 [gr-qc].

[72] L. Blanchet *et al.*, Phys. Rev. Lett. **74**, 3515 (1995).

[73] L. Blanchet *et al.*, Phys. Rev. Lett. **93**, 091101 (2004), arXiv:gr-qc/0406012 [gr-qc].

[74] A. Taracchini *et al.*, Phys. Rev. D **89**, 061502 (2014).

[75] M. Pürrer, Class. Quantum Grav. **31**, 195010 (2014).

[76] B. Allen *et al.*, Phys. Rev. D **85**, 122006 (2012), arXiv:gr-qc/0509116 [gr-qc].

[77] B. Sathyaprakash and S. Dhurandhar, Phys. Rev. D **44**, 3819 (1991).

[78] B. J. Owen and B. S. Sathyaprakash, Phys. Rev. D **60**, 022002 (1999), arXiv:gr-qc/9808076 [gr-qc].

[79] B. Allen, Phys. Rev. D **71**, 062001 (2005), arXiv:0405045 [gr-qc].

[80] J. Abadie *et al.*, Phys. Rev. D **85**, 082002 (2012), arXiv:1111.7314 [gr-qc].

[81] S. Babak *et al.*, Phys. Rev. D **87**, 024033 (2013).

[82] K. Cannon *et al.*, Astrophys. J. **748**, 136 (2012), arXiv:1107.2665 [astro-ph.IM].

[83] S. Privitera *et al.*, Phys. Rev. D **89**, 024003 (2014), arXiv:1310.5633 [gr-qc].

[84] A. Krolak and B. F. Schutz, Gen. Relativ. Gravit. **19**, 1163 (1987).

[85] P. A. R. Ade *et al.*, (2015), arXiv:1502.01589 [astro-ph.CO].

[86] M. Hannam *et al.*, Phys. Rev. Lett. **113**, 151101 (2014), arXiv:1308.3271 [gr-qc].

[87] S. Khan *et al.*, Phys. Rev. D (2016), accepted for publication, arXiv:1508.07253 [gr-qc].

[88] J. Veitch *et al.*, Phys. Rev. D **91**, 042003 (2015).

[89] J. Healy, C. O. Lousto, and Y. Zlochower, Phys. Rev. D **90**, 104004 (2014), arXiv:1406.7295 [gr-qc].

[90] B. Abbott *et al.*, (2016), `https://dcc.ligo.org/LIGO-P1500213/public`.

[91] C. K. Mishra *et al.*, Phys. Rev. D **82**, 064010 (2010), 1005.0304.

[92] T. G. F. Li *et al.*, Phys. Rev. D **85**, 082003 (2012), 1110.0530.

[93] C. Talmadge *et al.*, Phys. Rev. Lett. **61**, 1159 (1988).

[94] C. M. Will, Phys. Rev. D **57**, 2061 (1998), arXiv:9709011 [gr-qc].

[95] L. S. Finn and P. J. Sutton, Phys. Rev. D **65**, 044022 (2002), gr-qc/0109049.

[96] A. S. Goldhaber and M. M. Nieto, Phys. Rev. D **9**, 1119 (1974).

[97] S. Choudhury and S. SenGupta, Eur. Phys. J. **C74**, 3159 (2014).

[98] A. Tutukov and L. Yungelson, Nauchnye Informatsii **27**, 70 (1973).

[99] V. M. Lipunov, K. A. Postnov, and M. E. Prokhorov, Mon. Not. R. Astron Soc. **288**, 245 (1997), astro-ph/9702060.

[100] M. Dominik *et al.*, Astrophys. J. **806**, 263 (2015), arXiv:1405.7016 [astro-ph.HE].

[101] S. Sigurdsson and L. Hernquist, Nature **364**, 423 (1993).

[102] S. F. Portegies Zwart and S. L. W. McMillan, Astrophys. J. Lett. **528**, L17 (2000), astro-ph/9910061.

[103] C. L. Rodriguez *et al.*, Phys. Rev. Lett. **115**, 051101 (2015), arXiv:1505.00792 [astro-ph.HE].

[104] K. Belczynski *et al.*, Astrophys. J. **714**, 1217 (2010).

[105] M. Spera, M. Mapelli, and A. Bressan, Mon. Not. R. Astron Soc. **451**, 4086 (2015).

[106] B. Abbott *et al.*, (2016), `https://dcc.ligo.org/LIGO-P1500262/public`.

[107] C. Kim, V. Kalogera, and D. R. Lorimer, Astrophys. J. **584**, 985 (2003), arXiv:0207408 [astro-ph].

[108] W. M. Farr *et al.*, Phys. Rev. D **91**, 023005 (2015), arXiv:1302.5341 [astro-ph.IM].

[109] B. Abbott *et al.*, (2016), `https://dcc.ligo.org/LIGO-P1500217/public`.

[110] B. Abbott *et al.*, (2016), `https://dcc.ligo.org/LIGO-P1500222/public`.

[111] B. Abbott *et al.*, "Prospects for Observing and Localizing Gravitational-Wave Transients with Advanced LIGO and Advanced Virgo," (2015), LIGO-P1200087, VIR-0288A-12, arXiv:1304.0670v2 [gr-qc].

[112] B. Iyer *et al.*, *LIGO-India*, Tech. Rep. LIGO-M1100296 (2011).